

Properties of Silicon Ballistic Spin Fin-Based Field-Effect Transistor

D. Osintsev, V. Sverdlov, Z. Stanojevic, A. Makarov, J. Weinbub, and S. Selberherr

Institute for Microelectronics, TU Wien, Gußhausstraße 27-29, A-1040 Wien, Austria

We investigate the properties of ballistic fin-structured silicon spin field-effect transistors. The spin transistor suggested first by Datta and Das employs spin-orbit coupling to introduce the current modulation. The major contribution to the spin-orbit interaction in silicon films is of the Dresselhaus type due to the interface-induced inversion symmetry breaking. The subband structure in silicon confined systems is obtained with help of a two-band $\mathbf{k}\cdot\mathbf{p}$ model and is in good agreement with recent density functional calculations. It is demonstrated that fins with [100] orientation display a stronger modulation of the conductance as function of spin-orbit interaction and magnetic field and are thus preferred for practical realizations of silicon SpinFETs.

Introduction

The spectacular increase of computational speed and power of modern integrated circuits is supported by the continuing miniaturization of semiconductor devices' feature size. With scaling approaching its fundamental limits, however, the semiconductor industry is facing the challenge to introduce new innovative elements and engineering solutions and to improve MOSFET performance. Employing spin as an additional degree of freedom is promising for boosting the efficiency of future low-power nanoelectronic devices, with high potential for both memory (1) and logic (2) applications.

Silicon, the main element of microelectronics, possesses several properties attractive for spin-driven applications: it is composed of nuclei with predominantly zero spin and is characterized by small spin-orbit interaction. Because of that the spin relaxation in silicon is relatively weak, which results in large spin life time τ_s (3,4). In experiments, coherent spin propagation through an undoped silicon wafer of 350 μm thickness was demonstrated (5). Coherent spin propagation over such long distances makes the fabrication of spin-based switching devices in the near future increasingly likely.

The original proposal for the spin transistor by Datta and Das (6) employs the spin-orbit coupling for current modulation. The current modulation appears due to spin precession in an effective magnetic field caused by the spin-orbit interaction. Due to the structural inversion asymmetry induced by the effective electric field in the conducting channel, the strength of the spin-orbit interaction becomes a function of the gate voltage.

The electrons with a non-zero spin polarization are injected from the ferromagnetic source contact into the channel. The total current through the device depends on the relative angle between the magnetization direction of the drain contact \mathbf{e}_D and the electron spin polarization at the drain end of the conducting channel. Because the angle of the spin precession depends on the gate voltage, the total current through the device is modulated by the gate voltage.

The effective Hamiltonian of the spin-orbit interaction due to the structural-induced inversion asymmetry along the z-axis is usually considered to be of the Rashba type:

$$H_R = \alpha(p_x\sigma_y - p_y\sigma_x)/\hbar, \quad [1]$$

where α is the effective electric field dependent parameter of the spin-orbit interaction, $p_{x,y}$ are the electron momentum projections, and $\sigma_{x,y}$ are the Pauli matrices.

The weak strength of the spin-orbit interaction would be an obstacle to employ silicon for building a spin field-effect transistor similar to the one suggested by Datta and Das. As it is demonstrated in recent papers (7,8), the Rashba term [1] is indeed relatively small in silicon films inside SiGe/Si/SiGe heterostructures. Interestingly, in both perfect (001) silicon structures (7) and the silicon structures with interfacial disorder (8) there is another contribution to the spin-orbit interaction. Compared to the Rashba term, this contribution is approximately ten times larger, it depends strongly on the electric field, and it is described by the effective Hamiltonian

$$H_D = \beta(p_x\sigma_x - p_y\sigma_y)/\hbar, \quad [2]$$

which is of the Dresselhaus type. The value of the spin-orbit interaction β is estimated as $0.5 \cdot 10^{-12}$ eVcm at the built-in field $0.5 \cdot 10^5$ V/cm, in agreement with the experimental value (9). The spin-orbit interaction of such strength is sufficiently strong to investigate the possibility to build a silicon spin FET.

The stronger spin-orbit interaction, however, leads to an increased spin relaxation. The D'yakonov-Perel' mechanism is the main spin relaxation mechanism in systems with the degeneracy between the electron dispersion curves for the two spin projections lifted. In quasi-one-dimensional electron structures, however, the complete suppression of the spin relaxation was predicted (10).

Indeed, in case of the elastic scattering only back-scattering is allowed. Reversal of the electron velocity and momentum results in the inversion of the effective magnetic field direction in [2]. Therefore, the precession angle does not depend on scattering along the carrier trajectory in the channel, but is a function of the channel length only. Thus, spin-independent elastic scattering does not result in additional spin decoherence.

Model

We investigate the properties of ballistic fin-structured silicon spin field-effect transistors (SpinFETs). The SpinFET consists of the ferromagnetic source and drain electrodes connected by a silicon fin. The strength β of the spin-orbit interaction [2] depends on the electric field which is induced by applying a voltage to the gate. The Hamiltonian in the ferromagnetic regions which sandwich the silicon region are (11)

$$H_F^L = \frac{p_x^2}{2m_F} + h_0\sigma_z, \quad x \leq 0, \quad [3]$$

$$H_F^R = \frac{p_x^2}{2m_F} \pm h_0\sigma_z, \quad x \geq L, \quad [4]$$

where L is the channel length, m_F the effective mass in the contacts, σ_z is the Pauli matrix, and $h_0 = 2PE_F/(1+P^2)$, with $P < 1$ being the spin polarization and E_F the Fermi

energy. The plus/minus sign in [4] stands for parallel/anti-parallel configuration of the contact magnetization.

In order to circumvent the impedance mismatch problem between the metal electrodes and the semiconductor channel and to facilitate spin current injection in the channel (5) the delta-function barriers of strength U are introduced at the interfaces between the contacts and the channel (11). Contrary to (11), the spin-orbit interaction is taken in the Dresselhaus form [2] relevant for silicon (7,8). The Hamiltonian in the silicon region $0 < x < L$, for [100] and [110] fin orientations, is

$$H_S = \sum_n \frac{p_x^2}{2m_n} + \delta E_n - \frac{\beta}{\hbar} p_x \sigma_x + \frac{1}{2} g \mu_B B \sigma^*, \quad [100] \text{ fin}, \quad [5]$$

$$H_S = \sum_n \frac{p_x^2}{2m_n} + \delta E_n - \frac{\beta}{\hbar} p_x \sigma_y + \frac{1}{2} g \mu_B B \sigma^*, \quad [110] \text{ fin}, \quad [6]$$

where m_n is the n^{th} subband effective mass, δE_n is the band mismatch between the n^{th} subband in the channel and the source and drain contacts, B is the magnetic field, μ_B is the Bohr magneton, g is the Landé factor, and $\sigma^* = \sigma_x \cos \gamma + \sigma_y \sin \gamma$, with γ defined as the angle between the magnetic field and the fin direction.

Results

In our studies silicon fins have a square cross-section with (001) horizontal faces. The parabolic band approximation is not sufficient in thin and narrow silicon fins. In order to compute the subband structure in silicon fins we employ the two-band $\mathbf{k} \cdot \mathbf{p}$ model proposed in (12), which has been shown to be accurate up to 0.5eV above the conduction band edge (13). The resulting Schrödinger differential equation with the Hamiltonian (12), with the confinement potential appropriately added, is discretized using the box integration method and solved for each value of the conserved momentum p_x along the current directions using efficient numerical algorithms available through the Vienna Schrödinger-Poisson framework (VSP).

Fig.1 demonstrates the dependence of the subband minima as function of the fin thickness t , for the lowest four subbands. The fin orientation is along [110] direction. The dependence of the splitting between the unprimed subbands with decreasing t , which are perfectly degenerate in the effective mass approximation, is clearly seen. Splitting between the valleys in a [100] fin can be ignored (14). In contrast, the dependence of the effective mass of the ground subband in [100] fins on t is more pronounced as compared to [110] fins. Results of density-functional calculations (14) confirm the mass dependences obtained from the $\mathbf{k} \cdot \mathbf{p}$ model (Fig.2).

With the values of the effective masses and subband offsets obtained we study the conductance G through the system, for parallel and anti-parallel configurations of the contacts. Fig.3 shows the dependence of tunneling magnetoresistance (TMR) defined as

$$\text{TMR} \equiv \frac{G_{\uparrow\uparrow} - G_{\uparrow\downarrow}}{G_{\uparrow\downarrow}}, \quad [7]$$

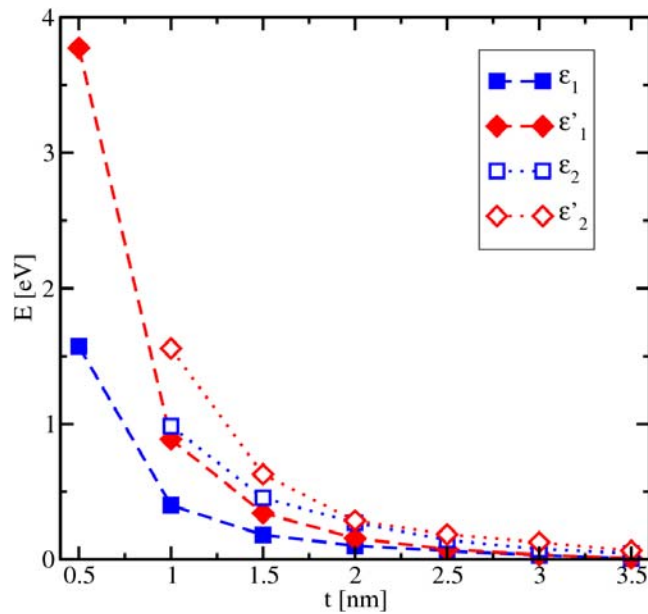


Figure 1. Subband minima as a function of [110] fin thickness t .

for [100] and [110] oriented fins with $t=1.5\text{nm}$ on the value of spin-orbit interaction. Fins of [100] orientation display stronger dependence on β and are thus preferred for practical realizations of silicon SpinFETs. This is due to the fact that the scale of the TMR dependence on the spin-orbit interaction is determined by the characteristic wave vector $k_D = m_n \beta / \hbar^2$. Because the effective mass in [110] fins is substantially smaller than in [100] structures, one needs a larger variation of β in order to acquire the same variation of k_D .

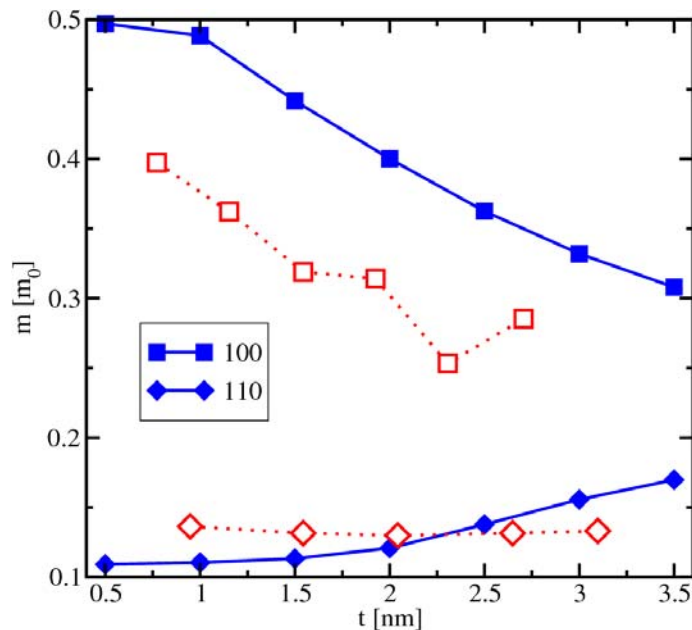


Figure 2. Ground subband effective mass dependence on t in [100] and [110] fins obtained with the $\mathbf{k}\cdot\mathbf{p}$ method (filled symbols) and with the first-principle calculations (14) (open symbols). The discrepancy between the curves is due to surface passivation and structure relaxation present in the first principles calculations (14) but not in $\mathbf{k}\cdot\mathbf{p}$.

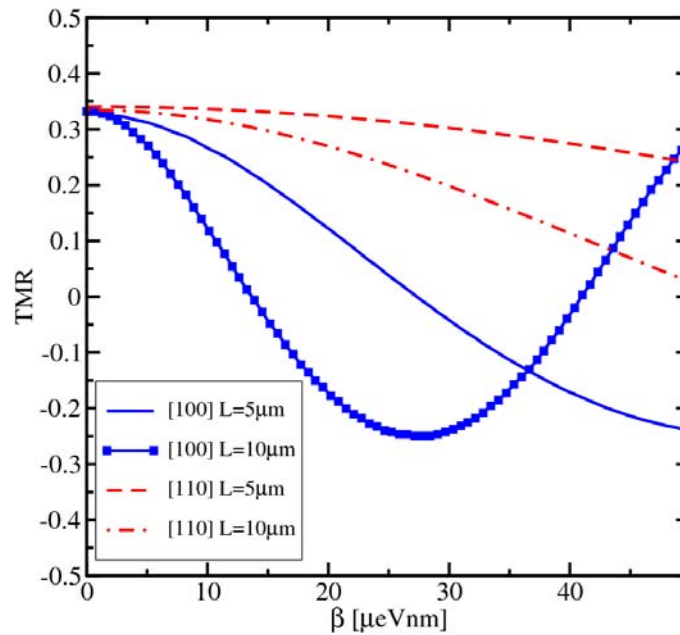


Figure 3. TMR dependence on the value of the Dresselhaus spin-orbit interaction parameter for $t=1.5\text{nm}$, $B=0\text{T}$, $P=0.4$, $z=5$ ($z = U\sqrt{2m_f/E_f}/\hbar$).

Thanks to the Dresselhaus form of the spin-orbit interaction, the TMR of [110] fins is most affected by the magnetic field along the transport direction (Fig.4), while the magnetic field orthogonal to the transport direction influences the TMR of [100] fins (Fig.5). Also, the TMR in [100] fins is most modified by the external magnetic field, which provides an additional option to tune the performance of the silicon SpinFET.

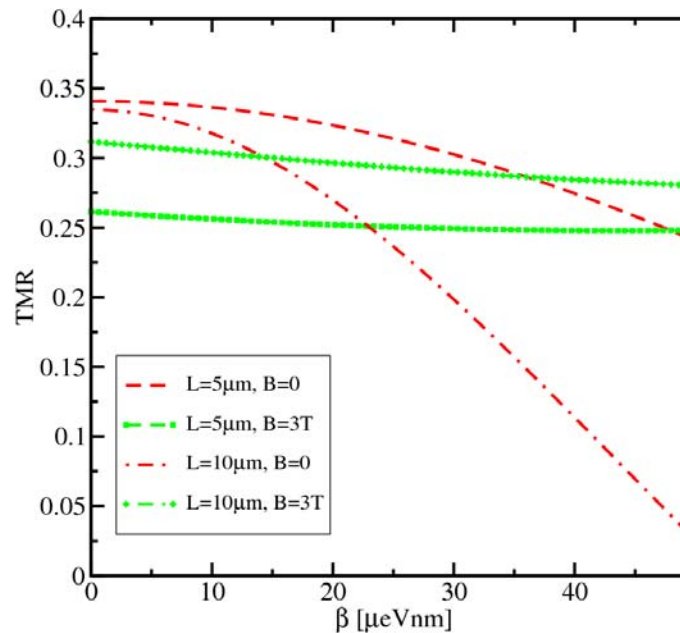


Figure 4. TMR dependence on the value of the Dresselhaus spin-orbit interaction parameter for a [110] fin with $t=1.5\text{nm}$, ($P=0.4$, $z=5$) in a magnetic field $B=3\text{T}$ parallel to the transport direction.

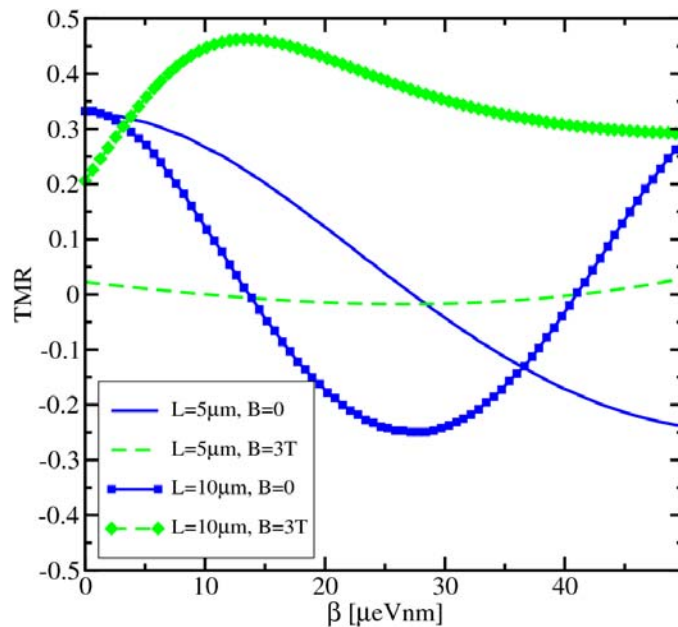


Figure 5. TMR dependence on β for a [100] fin with $t=1.5\text{nm}$, ($P=0.4$, $z=5$) in a magnetic field $B=3\text{T}$ in [010] direction.

Conclusion

A possibility to build a SpinFET by using silicon fins is investigated. The spin-orbit interaction due to the interface-induced inversion symmetry breaking is taken in the Dresselhaus form. It is shown that [100] fins are more suitable for practical realizations of silicon SpinFETs.

Acknowledgments

This work is supported by the European Research Council through the grant #247056 MOSILSPIN.

References

1. S.Parkin, M.Hayashi, L.Thomas, *Science* **320**, 190 (2008).
2. T.Marukame, T.Inokuchi, M.Ishikawa, H.Sugiyama, Y.Saito, IEDM 2009, pp.1-4.
3. J.L.Cheng, M.Wu, J.Fabian, *Phys. Rev. Lett.* **104**, 016601 (2010).
4. S.P.Dash, S.Sharma, J.C.Le Breton, H.Jaffrès, J.Peiro, J.-M.George, A.Lemaître, R.Jansen., arXiv:1101.1691 (2011).
5. B.Huang, D.Monsma, I.Appelbaum, *Phys. Rev. Lett.* **99**, 177209 (2007).
6. S.Datta, B.Das, *Appl.Phys.Lett.* **56**, 665 (1990).
7. M.O.Nestoklon, E.L.Ivchenko, J.-M.Jancu, P.Voisin, *Phys.Rev.B* **77**, 155328 (2008).
8. M.Prada, G.Klimeck, R.Joynt, *Birk & NCN Publications*, paper 516 (2009).
9. Z.Wilamowski, W.Jantsch, *Phys. Rev. B.* **69**, 035328 (2004).
10. A.Bournel, P.Dollfus, P.Bruno, P.Hesto, *European Phys. J. Appl. Phys* **4**, 1 (1998).
11. K.M.Jiang, R.Zhang, J.Yang, C.-X.Yue, Z.-Y.Sun, *IEEE T-ED* **57**, 2005 (2010).
12. G.L.Bir, G.E.Pikus, *Symmetry and Strain-Induced Effects in Semiconductors*, J.Wiley & Sons, NY, 1974.
13. V.Sverdlov, O.Baumgartner, T.Windbacher, S.Selberherr, *J.Computational Electron.*, **8**, 192 (2009).
14. H.Tsuchiya, H.Ando, S.Sawamoto, T.Maegawa, T.Hara, H.Yao, M.Ogawa, *IEEE T-ED* **57**, 406 (2010).